

System Representation for the Control System of the Follow-up Mechanism on the Marine Gyro Compass

Sang-Jib Lee*

ABSTRACT

It does not seem necessarily practicable to keep the system always in optimal condition, although the control system of the follow-up mechanism on the most marine gyro compasses is to be adjusted by the operator through the gain adjustment. Sometimes a sustained oscillation or an incorrect gyro reading occurs to the system. For such a system any systematical research or theoretical basis of the guide for the optimal gain adjustment has not been reported yet. As a basic investigation of the theoretical system analysis to solve the problems concerned, the author attempts in this paper to express the system in a mathematical model deduced from the results of the theoretical approach and the experimental observation of each element contained in the follow-up mechanism of Hokshin D-1 gyro compass, and to constitute an over-all closed loop transfer function. This function being reverted to a fourth order linear differential equation, the first order simultaneous differential equations are obtained by means of the state-variables. The latter equations are solved by the Runge-Kutta method with digital computer. By comparing the characteristic of the simulated over-all output with that of the experimental result, it is shown that both outputs are nearly consistent with each other. It is also expected that the system representation proposed by this paper is valid and will be a prospective means in a further study on the design and optimal adjustment of the system.

I. INTRODUCTION

The gyro compass reading on the marine gyro compass depends upon both the north-directing function of the sensitive part itself and the direction-indicating function of the follow-up mechanism. The accuracy of the north-directing function is governed by the latitude error, speed error, ballistic deflection error, rolling error, gimbal error, balancing error and other mechanical and electrical errors. These errors are minimized by virtue of the newly-developed supporting system of the sensitive part, error adjusting mechanism, automatic error correcting system and other compensating appliances. Nowadays it is possible to minimize the sum of these errors to be less than 0.1 degree¹⁾.

On the other hand, as to the follow-up control system few researches of the functional analysis have been reported, while several different types of electro-electric elements of the

* Regular Member, Korea Merchant Marine College.

follow-up mechanisms are in practical use.

The follow-up control system governs the direction-indicating function, only through which gyro reading is shown to the users and transmitted to the repeaters used in conjunction with other nautical instruments and facilities. The follow-up actions are to be classified into two kinds; one is wandering-follow whose actuating signal generation is caused by the motion of the sensitive part when it is under north-seeking or when it contains the transient error in north-directing function, and the other is keeping-follow whose actuating signal generation is caused by the motion of the stationary part and keeps the direction-indicating up to the north-directing of the sensitive part, when the ship is under altering her course or turning her head due to rolling or pitching by the external forces such as wind, wave, etc. In the former case, a relative angular displacement in azimuth between gyro sphere and container(hereinafter this displacement is referred to as a deflection) is motivated by the result of the north-seeking of the sensitive part. In the latter case, a similar deflection is motivated by the mechanical resistance between stationary part and follow-up mechanism. In general, it seems possible for these follow-up actions to happen separately or simultaneously. But as, under normal operating state, wandering-follow does not happen, we are interested in only the keeping-follow action. This action is assumed to happen almost continually since there always occurs the stationary part motion about the vertical axis when the ship is under way.

The most follow-up system currently used in marine gyro compasses are to be adjusted by the gain adjustments so that the stability and accuracy of the system may be assured. But it does not seem necessarily practicable to keep the system in optimally adjusted state. If the gain is set high, the rapidity of response may increase while the stability of the system decreases, sometimes resulting in a sustained oscillation of the system. If the gain is set too low, steady state errors may occur while the stability increases, introducing errors in direction-indicating function. Therefore, to a design new type of the follow-up system or to present a guide of the optimal gain adjustment of it, theoretical analysis of the problems concerned should be studied systematically.

As a basic investigation, in this paper, the author attempts to express in a mathematical model the follow-up system of Hokshin D-1 gyro compass as an example, by constituting an over-all transfer function from the results of the theoretical approach and experimental observation of each element contained therein. The characteristic of the simulated over-all outputs by the digital computer is obtained and that of the observed over-all outputs is recorded. By the comparison of the transient dynamic characteristics of both outputs, it is proved that the system representation proposed in this paper is valid and may be very useful in continuing the study on this field.

This paper is based on such assumptions as follows:

1. The normal operating state is referred to a state when the sensitive part is settled. The keeping follow is assumed to happen only under normal operating state without any mechanical or electrical defect.

2. The effects of coulomb friction and mechanical backlashes such as those of gears and spring linkages on the system are to be disregarded.
3. The value of deflection is thought to be less than 5 degrees.

II . TRANSFER FUNCTION OF THE FOLLOW-UP SYSTEM

II - 1. CONSTRUCTION OF THE FOLLOW-UP SYSTEM

Among the different types of the system whose actuating signals depend upon the variation of the liquid resistance, Hokshin D-1 gyro compass is examined. When the gyro compass of this type is under normal operating state, the gyro sphere is supported by the liquid in the follow-up container. The center of gyro sphere is stabilized by the centering pin whose top tip is secured to the ceiling center of the container (Fig.1)²⁾.

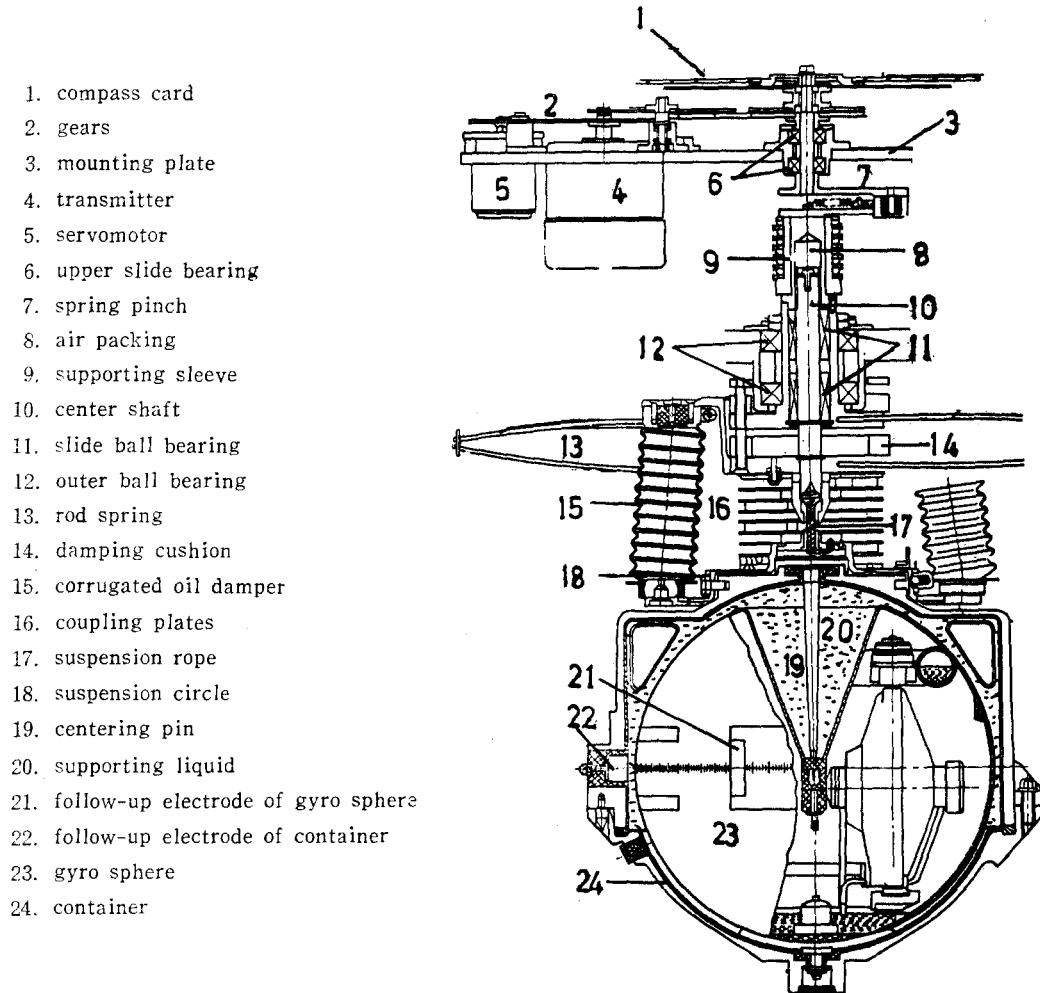
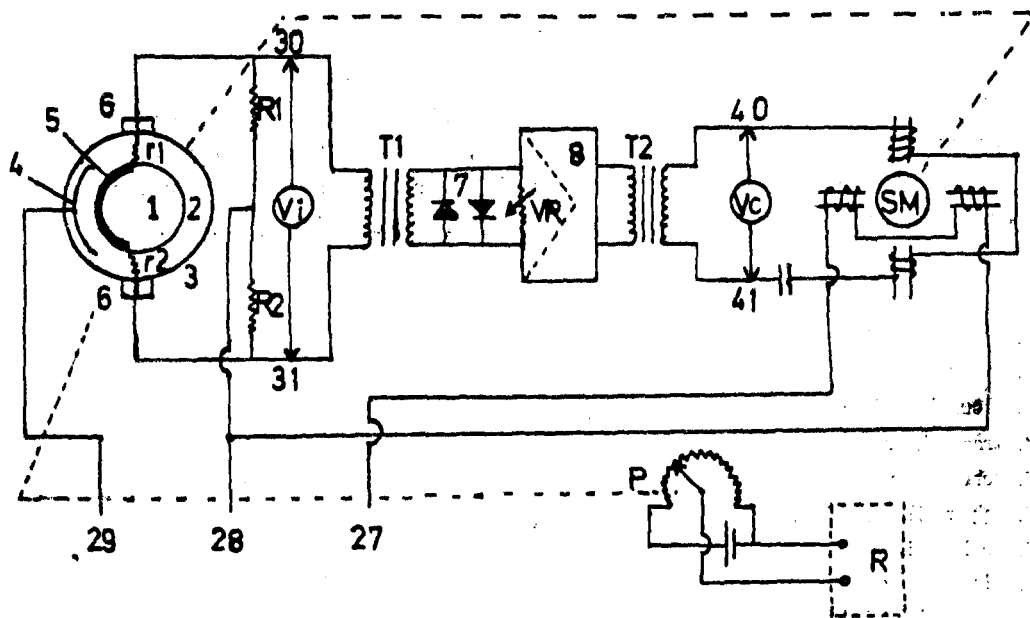


Fig.1. Schematic diagram of container and its suspension mechanism.

If the gyro sphere or the stationary part turns, the follow-up mechanism has the deflection against the gyro sphere. This deflection is to be detected and converted into the signal voltage by the error detector comprising a Wheatstone bridge resistance circuit, and this voltage is amplified and serves to drive the servomotor in such a manner as to constantly keep the container in alignment with the gyro sphere.



- | | | |
|---------------------------|-----------------------------|---------------------|
| 1. gyro sphere | 5. electrode of gyro sphere | P. potentiometer |
| 2. supporting liquid | 6. follow-up electrodes | R. pen recorder |
| 3. container sphere | 7. double-diode clipper | Vi. signal voltage |
| 4. electrode of container | 8. amplifier | Vc. control voltage |

Fig. 2. Schematic wiring diagram of the follow-up system and output measuring installation

Fig. 2 Shows the Wheatstone bridge circuit consisting of the four electric resistances; the r_1 and r_2 are variable liquid resistances, an electrically conducting fluid consisting of the distilled water, glycerin and benzoic acid, and the remaining R_s are the fixed resistances equal in value³⁾. The azimuthal displacement between the gyro sphere and the container introduces the unbalance of the resistances r_1 and r_2 , which in turn leads to the electric voltage between terminals 30-31. This signal voltage becomes the output voltage, the driving force of the servomotor, by way of the transformer T_1 , amplifier and transformer T_2 . The servomotor is to be controlled by the value and phase of this voltage.

II-2. TRANSFER FUNCTION OF THE FOLLOW-UP SYSTEM

The follow-up system consists of five elements: error detector(comparator, transducer), amplifier, servomotor, gears and container sphere. The relationship of these elements are

shown in Fig. 3.

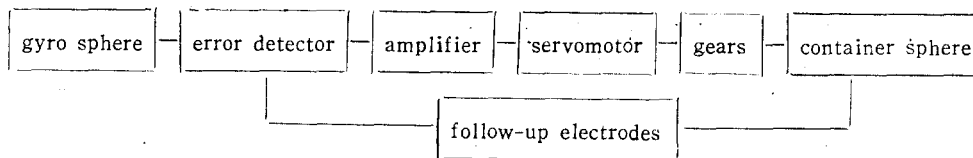


Fig. 3. Over-all block diagram showing the relationships of the elements.

1) Error detector and amplifier

The error detector generally used on the ship's gyrocompass serves as both comparator and transducer at the same time. Such error detectors can be divided into two types; one comprises the electro-induction differential transformer with E-shaped iron core and armature where the error signal is derived by the relative displacement of the transformer to the armature, and the other comprises Wheatstone bridge circuit where the error signal is derived by the variation of the liquid resistances. The latter is applied to the follow-up system of the Hokshin D-1 gyro compass. The gain constant of this error detector K_f (voltage gradient of the transducer) is to be determined through the theoretical approach and experimental results. Referring to Fig. 2, the current I_g through the terminals 30-31 may be written as

$$I_g = \frac{(r_1 - r_2) \cdot R \cdot E}{X_L(r_1 + R)(r_2 + R) + r_1 \cdot R(r_2 + R) + r_2 \cdot R(r_1 + R)} \dots\dots\dots(1)$$

where r_1 and r_2 are the liquid variable resistances, R is the fixed resistance ($R = R_1 = R_2$), X_L is the primary coil reactance of transformer T_1 , and E is the voltage between the terminals 28-29. If there is no deflection, r_1 and r_2 are in the state of equilibrium to each other and I_g becomes zero. If, on the other hand, there is a little deflection, I_g is expressed as follows. By giving consideration only to the geometric gap between the follow-up electrodes facing each other, it can not be concluded that the liquid resistance is proportional to the deflection. But with a little value of deflection, the variation of resistance is assumed to be proportional to that of the deflection. Therefore, in case there is a little deflection, r_1 and r_2 become $r_1 = r + \Delta r$, $r_2 = r - \Delta r$ respectively. Inserting these modified values of resistances into Eq. (1), we have

$$I_g = \frac{2 \cdot E \cdot \Delta r}{X_L \{ (r + R)^2 - \Delta r^2 \} + 2 \cdot (r^2 + Rr^2 - \Delta r^2)}$$

$$\doteq \frac{2 \cdot E \cdot \Delta r}{X_L (r + R)^2 + 2r \cdot (r + R)} \dots\dots\dots(2)$$

Hence the voltage V_i between the terminals 30-31 (this will be referred to as a signal voltage) can be written

$$V_i = \frac{2 \cdot E \cdot X_L}{X_L (r + R)^2 + 2r \cdot (r + R)} \cdot \Delta r = K \cdot \Delta r$$

where
$$K = \frac{2 \cdot E \cdot X_L}{X_L (r + R)^2 + 2r \cdot (r + R)}$$

As $\Delta r / \Delta D$ is to be constant, we have

$$V_i = K_f \cdot \Delta D \dots\dots\dots(3)$$

where ΔD = deflection angle(infinitesimal)

$$K_f = K \cdot \Delta r / \Delta D$$

Referring to Eq. (3), the signal voltage is proportional to the deflection. As the dimension of K is ampere, that of K_f is to be volt/unit deflection, which represents the gradient of the transducer. If the theoretical value of K is constant, that of K_f is also constant. In practice, however, V_i is varied by the amplification factor K_a . Therefore, it is desirable that K_f is to be expressed as a function of K_a , which is determined by examining the characteristic of the signal-deflection and that of output voltage-deflection. In measuring the signal voltage V_i and output voltage V_c (this is the voltage between the terminal 40-41 and is to be the servomotor control voltage), the initial deflection is set to 5 degrees and the variable resistor(VR) of the amplifier is successively adjusted to vary the output voltages in step values(hereinafter this is referred to as an initial setting). In each case,

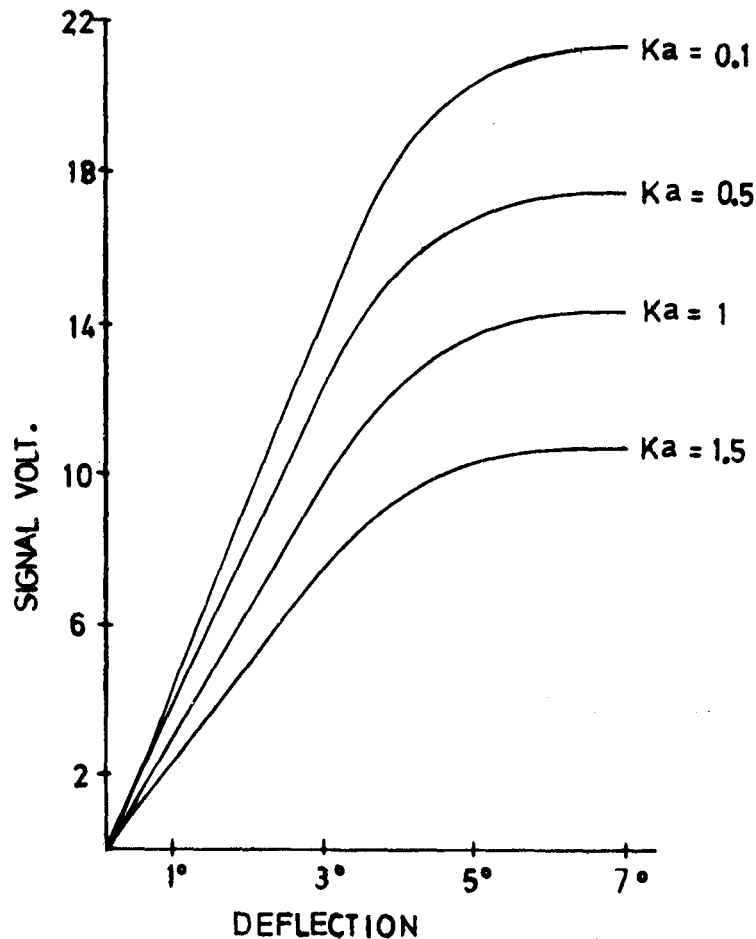


Fig. 4. Signal voltage vs. deflection by K_a .

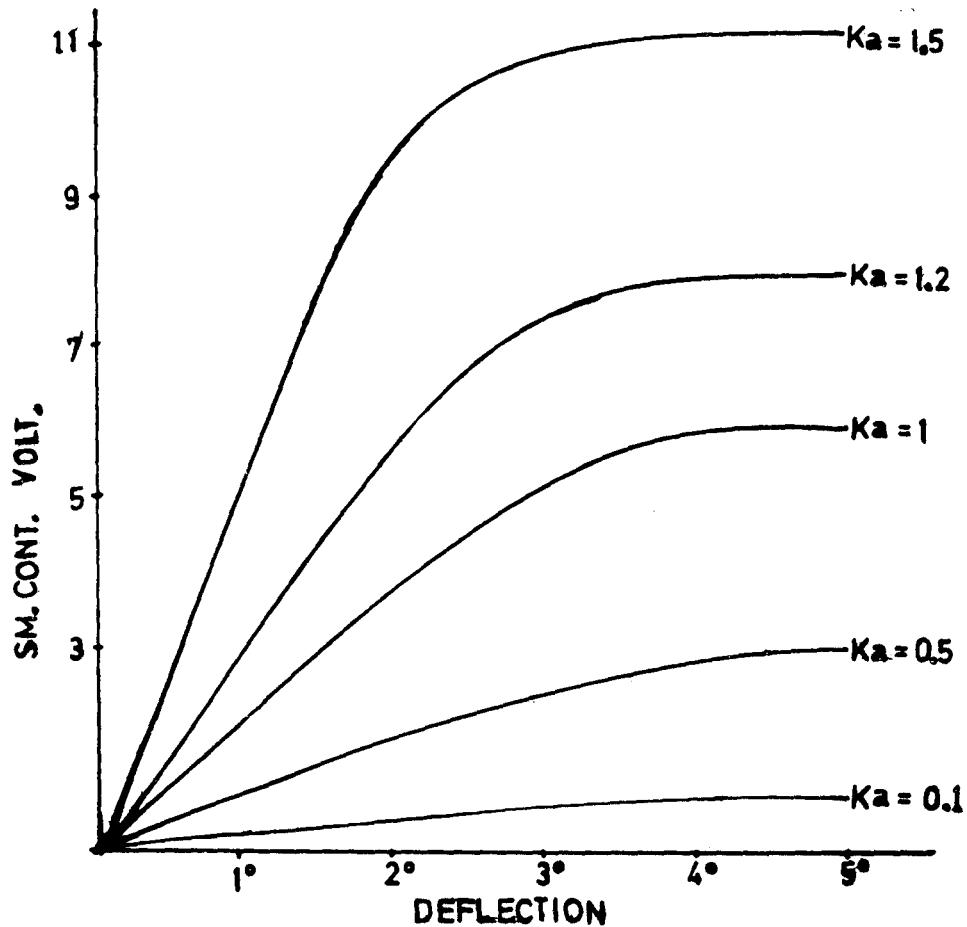


Fig. 5. Servomotor control voltage vs. deflection by K_a .

the voltages V_i and V_c are measured simultaneously by decreasing the deflection, and their characteristics by each specific K_a are shown in Figs 4. and 5. Referring to Figs. 4 and 5, it is found that both voltages are governed not only by the deflection but also by K_a , i. e., for a given deflection, V_i decreases with the increasing of K_a due to the mutual induction of transformer T_1 , while, for a given K_a , if the deflection is greater than 5 degrees, both voltages become limited by the effect of the secondary voltage of T_1 which is clipped by the diodes. But, for a given K_a , if the deflection is less than 5 degrees, both voltages are nearly in proportion to the deflection. In the range excluding the clipped section of each line, though the characteristic lines are not straight, they are to be linearized. In this range, the value of K_a for each initial setting state is obtained by dividing the value of slope representing output voltage characteristic by that of the slope representing signal voltage characteristic correspondingly for each case, and these are tabulated as in Tab. 1.

Tab. 1. Signal voltage, output voltage and Ka.

| | | | | | | | | | | | |
|--|-----|-----|-----|-----|-----|-----|-----|-----|------|-----|------|
| output voltage under initial setting state | 11 | 10 | 9 | 8 | 7 | 6 | 5 | 4 | 3 | 2 | 1 |
| output voltage per unit deflection | 4.7 | 4.1 | 3.4 | 2.7 | 2.1 | 1.7 | 1.4 | 1.1 | 0.8 | 0.5 | 0.1 |
| signal voltage per unit deflection | 2.5 | 3.1 | 3.5 | 4 | 4.1 | 4.2 | 4.3 | 4.4 | 4.5 | 4.6 | 4.3 |
| amplification factor Ka | 1.5 | 1.3 | 1 | 0.7 | 0.5 | 0.4 | 0.3 | 0.2 | 0.17 | 0.1 | 0.06 |

Referring to Tab. 1, the characteristic line of signal voltage versus Ka can be drawn as in Fig. 6. As this line seems almost linear, its slope, Vi/unit deflection (gradient of transducer), can be expressed as $4.5 - (4/3) \cdot Ka$ (volt/deg), where Ka is the amplification factor.

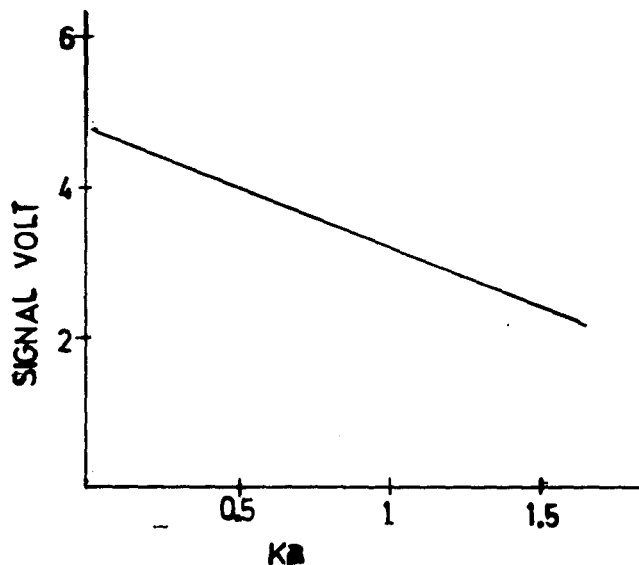


Fig. 6. Signal voltage vs. Ka.

Hence, the coefficient of the error detector Kf can be written as

$$Kf = \{4.5 - (4/3) \cdot Ka\} \cdot 57.3 \text{ (volt/rad)} \dots \dots \dots (4)$$

Consequently the output voltage Vc can be written as

$$Vc = Ka \cdot Kf \\ = \{4.5 \cdot Ka - (4/3) \cdot Ka^2\} \cdot 57.3 \text{ (volt/rad)} \dots \dots \dots (5)$$

As previously described, the output voltages are clipped if the deflections are over about 5 degrees. Under the initial setting state with the maximum turn of the gain knob, the output voltage reaches near 11 volts. Under the similar state with the minimum turn of it, that voltage drops nearly less than 1 volt. In practice, in the former case, the system encounters a sustained oscillation, while in the latter case the servomotor does not work. Referring to Tab. 1, the values of output voltages range from 0.3 up to 4.7 (volt/deg) and those of the signal voltages do from 2.5 up to 4.7 (volt/deg). Also the values of

Ka range from 0.03 up to 1.5.

2) Servomotor

There are some non-linear properties in dynamic characteristics of the servomotor, such as input impedance depending on the control voltage, damping factor on the angular velocity and control voltage, torque on the temperature and the control voltage, etc. But within the operational range where the torque-r.p.m. characteristic is approximated as linear, a transfer function can be deduced. Noticing that the torque is a function of the angular velocity and control voltage, the author has the transfer function of the servomotor, whose constants are determined from the experimental results.

In the neighborhood of the operating equilibrium point, the a-c two phase motor can be characterized by the equation⁵⁾.

$$T = \frac{\partial T}{\partial \theta} \theta + \frac{\partial T}{\partial I_m} I_m \dots\dots\dots(6)$$

where T = torque of the servomotor
 I_m = control field current
 θ = angular velocity.

If there is no external load and viscous friction, Eq. (6) can be written as

$$\begin{aligned} J_m \frac{d^2 \theta}{dt^2} &= \frac{\partial T}{\partial \theta} \cdot \frac{d\theta}{dt} + \frac{\partial T}{\partial I_m} \cdot I_m \\ &= \frac{\partial T}{\partial \theta} \cdot \frac{d\theta}{dt} + \frac{\partial T}{\partial I_m} \cdot \frac{\partial I_m}{\partial V_c} \cdot V_c \\ &= \frac{\partial T}{\partial \theta} \cdot \frac{d\theta}{dt} + \frac{\partial T}{\partial V_c} \cdot V_c \dots\dots\dots(7) \end{aligned}$$

where J_m = inertia moment of the rotary part of the servomotor
 θ = angular displacement
 V_c = control voltage

Substituting $-D$ for $\frac{\partial T}{\partial \theta}$ and K for $\frac{\partial T}{\partial V_c}$, and taking the Laplace transform on both sides of Eq. (7), and assuming the zero initial conditions. we can write the transfer function of servomotor $G_m(s)$ as

$$G_m(s) = \frac{K_m}{S(T_m S + 1)} \dots\dots\dots(8)$$

where $K_m = K/D$, $T_m = J_m/D$.

The values of K_m and T_m can be determined by the torque-r.p.m. characteristic curves. In the first step of the torque experiments, within the acting range of the servomotor control voltage(11 volt), the angular velocity variation is investigated as follows:

Setting K_a value in maximum(1.5), the initial deflection is forced to be set to a selected value and then the system is freed to the normal operating condition, meanwhile the maximum r.p.m. during the transient state is read by the tachometer(a frictionless phototachometer made in Yokogawa electric works, type 2607). For various initial deflections up to 5 degrees, maximums of angular velocities are measured and tabulated as in table 2.

from which is found that the larger is the initial deflection, the greater the maximum r.p.m. and the over-all maximum angular velocity is up to 2,500 r.p.m. at maximum deflection. Thus within 5 degrees, the angular velocity range is within 2,500 r.p.m.

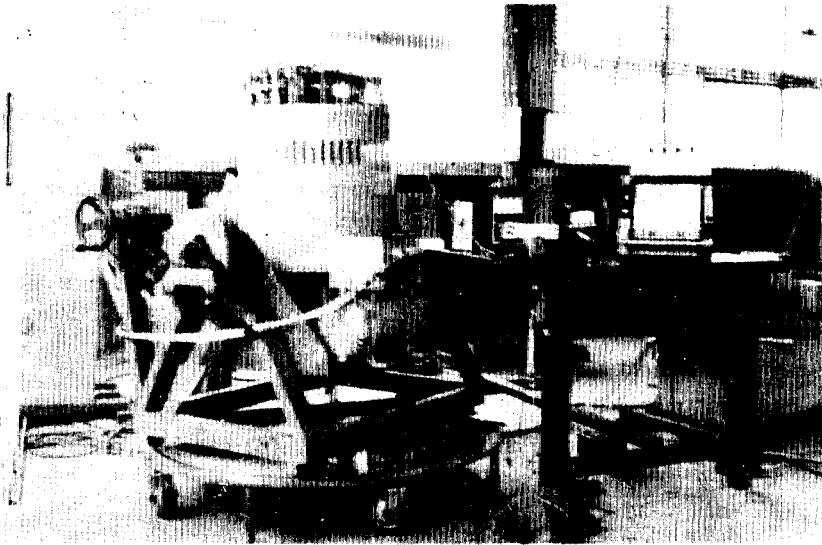


Fig. 7. General view of experimental installations

Tab. 2. Deflection, maximum r. p. m. of servomotor.

| deflection angle | r. p. m. |
|------------------|----------|
| 5 | 2,500 |
| 4 | 2,000 |
| 3 | 1,800 |
| 2 | 1,200 |
| 1 | 600 |
| 0.5 | 45 |

The servomotor torque experiments are accomplished as follows: Separating the servomotor from the system, and securing it to a bracket on the fixed stand so that the rotary axle may be kept in horizontal level, a pulley(2 cm in diameter) is fitted to one end of the rotor axle. A fine thread is hung on that pulley and one end of the thread is fastened to the spring balance and the other to the weight selectable.

Though the servomotor is separated from the system mechanically, it is still kept in normal operating state electrically so that the control voltage of servomotor may be controlled by varying K_a .

The control voltage keeping up the anticipated one by adjusting K_a , the scale of the spring balance together with the tachometer reading is read. The difference between the value of weight hung and that of the spring balance multiplied by the semi-diameter of the pulley is assumed to be the torque to the indicated r.p.m. Same procedures of the measurements and calculations are made under various values of weights and voltages. The torque-r.p.m. characteristic curves by each control voltages are obtained as in Fig. 8.

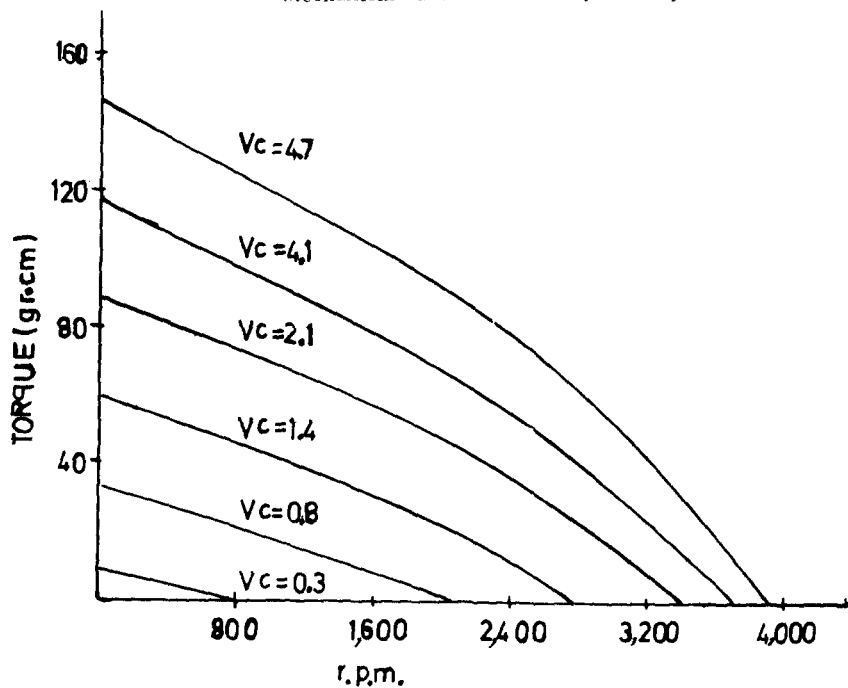


Fig. 8. Torque vs. r.p.m. by Vc.

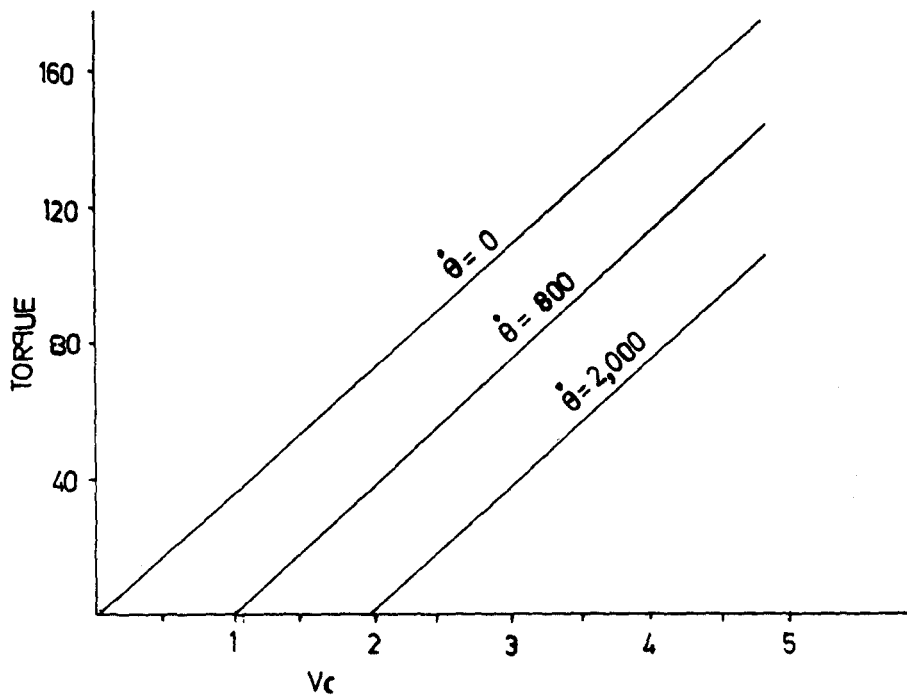


Fig. 9. Torque vs. Vc by r.p.m.

From these curves the torque-control voltage characteristic curves can be deduced as in Fig 9. Referring to Fig. 8, torque-r.p.m. characteristic curve to a given control voltage is assumed to be a straight line within 2,500 r.p.m. As the slope $(\frac{\partial T}{\partial \theta} = -D)$ of these lines are different by the control voltages, the slope can be expressed as

$$D = -(0.12 + \langle 0.024/57.3 \rangle V_c) \text{ (gr}\cdot\text{cm/rad/sec)} \dots\dots\dots(9)$$

Referring to Fig.9, the slope $(\frac{\partial T}{\partial V_c} = K)$ is shown nearly constant regardless the value of V_c and expressed as $K=30.5$.

Consequently, $K_m = 30.5 / (0.12 + \langle 0.024/57.3 \rangle V_c)$, $T_m = 0.03 / (0.12 + \langle 0.024/57.3 \rangle V_c)$ ※

Hence the transfer function of the servomotor $G_m(s)$ can be written as

$$G_m(S) = \frac{30.5 / (0.12 + \langle 0.024/57.3 \rangle V_c)}{S [\{ 0.03 / (0.12 + \langle 0.024/57.3 \rangle V_c) \} S + 1]} \dots\dots\dots(10)$$

3) Gear

The servomotor and the azimuth gear concentric with the compass card is linked by reduction gears in such a way that one degree of compass card turning refers to seven revolutions ($7 \times 3.14 \times 2$ radians) of the servomotor. Therefore, the compass card deflection C_d in radian can be written as

$$C_d = 1 / (7 \times 2 \times 3.14 \times 57.3) \times S_d$$

where S_d is the servomotor turning angle in radian.

Hence the coefficient of the gear train K_g can be written as

$$K_g = 1 / (7 \times 2 \times 3.14 \times 57.3) \dots\dots\dots(11)$$

4) Container(follow-up container) sphere

The container sphere is supported by the several different elastic elements which provide horizontal and vertical flexibility for the container and two sets of bearings which do free movement and guidance about the vertical axis of the stationary part for it. Referring to Fig. 1, there are, between the container and center shaft, four vertical corrugated oil dampers arranged in quadrantal equi-angular points and seven horizontal coupling plates whose limbs make concentric circles about the suspension rope, and between the bottom of center shaft and that of supporting sleeve, 4 bundles of horizontal rod springs stretched radially in quadrantal equi-angular directions, and on the top part of the sleeve, an air packing, and on the lower part of the center shaft, damping cushion, and between lower part and upper part of the follow-up mechanism, a horizontal-coil spring pinch. The arrangement of these elements provides shock-absorbing for the system so that the transmission of the vertical impact and swing effect from a ship motion to the container sphere may be diminished. Therefore, from the view point of dynamics, the container sphere itself is assumed to be supported by a coil spring which has vertical and horizontal elasticity, i.e., a torsional spring.

※ The inertial moment of the rotary part of the servomotor about its spin axis is determined from the observed equations comprising the time constants measured by varying K_a .

In normal operating state, the servomotor driving force is applied to the compass card directly through the gear train and then the container sphere is to turn with a horizontal elasticity. Therefore, the azimuthal displacement of the compass card is to be taken as an input and that of the container sphere as an output.

Consequently, when a torque is applied to the compass card, the supporting system of the container sphere is characterized by the equation ^{(6), (7), (8)}

$$T_i = K_c(\theta_i - \theta_o) \dots \dots \dots (12)$$

where T_i = applied torque tending to twist the supporting mechanism

K_c = torsional spring rate of the supporting mechanism.

θ_i = angular displacement of the compass card

θ_o = angular displacement of the container sphere.

As previously described, within the container sphere, the gyro sphere is located by the centering pin. The space between both spheres is filled with the supporting liquid. During normal operating state the gyro sphere does not touch the inside wall of the container sphere and the travelling swirl effect inward from the inside wall of the container sphere diminishes rapidly by increasing the gap between both spheres and its effect is negligible in practical use. Therefore, the contents contained in the container sphere can be assumed to be a liquid filled in a hollow sphere shell and this liquid is to oscillate about the vertical diameter during follow-up action.

Thus the right side of Eq. (12) can be assumed to equilibrate with two forces: one (F_1) is due to the mechanism of the container sphere and its supporting mechanism and the other (F_2) is due to the liquid filled in the container sphere. These forces are expressed respectively as follows:

$$F_1 = J \frac{d^2\theta_o}{dt^2} + B \frac{d\theta_o}{dt}$$

where J = inertial moment of the container supporting system

B = coefficient of the mechanical friction

$$F_2 = (4/3)\pi\rho a^4\beta^{-1} \frac{d^2\theta_o}{dt^2} + (8/3)\pi\mu a^4\beta \frac{d\theta_o}{dt}$$

where ρ = density of the supporting liquid

a = inner semi-diameter of the container sphere shell

μ = viscous coefficient of the supporting liquid

$\beta = \sqrt{\sigma v/2}$ (σ = oscillation frequency of the supporting liquid,

$v = \frac{\mu}{\rho}$; coefficient of kinematic viscosity of that liquid).

Therefore, the container sphere motion equation can be written as

$$J_c \frac{d^2\theta_o}{dt^2} + D_c \frac{d\theta_o}{dt} + K_c\theta_o = K_c\theta_i \dots \dots \dots (13)$$

$$\begin{aligned} \text{where } J_c &= J + (4/3)\pi\rho a^4\beta^{-1} \\ D_c &= B + (8/3)\pi\mu a^4\beta \end{aligned}$$

Taking the Laplace transform on the both sides of Eq.(13) and assuming the zero initial condition, we have the transfer function of the container $G_m(S)$

$$G_m(S) = \frac{\theta_c(S)}{\theta_i(S)} = \frac{K_c}{J_c S^2 + D_c S + K_c} = \frac{W_n^2}{S^2 + 2\varphi W_n S + W_n^2} \dots\dots\dots (14)$$

where $W_n = \sqrt{K_c/J_c}$: angular velocity of the container mechanism in free oscillation
 $\varphi = D_c / (2\sqrt{J_c \cdot K_c})$: damping factor.

As it is neither easy nor inevitable to determine the value of each factor contained in the above equations separately, the author attempts to deduce the coefficients in Eq. (14) directly from the results of the container dynamic motion observation.

The axle of the potentiometer comprising the rotary solenoid rheostat(10 K ohm) and d-c 22 volt power source is geared to the center of the bottom end of the container sphere and the mechanical friction due to the potentiometer installation is minimized so that the voltage variation proportional to the container motion about the vertical axis can be measured and recorded by the pen recorder(Rectigraph 8S, by San-ei instrument Co.). After the gyro compass reaches normal operating state, the circuit is opened and the servomotor is disconnected from the compass and then a step input is applied to the container mechanism by turning the compass card and its output response is illustrated in Fig. 10.

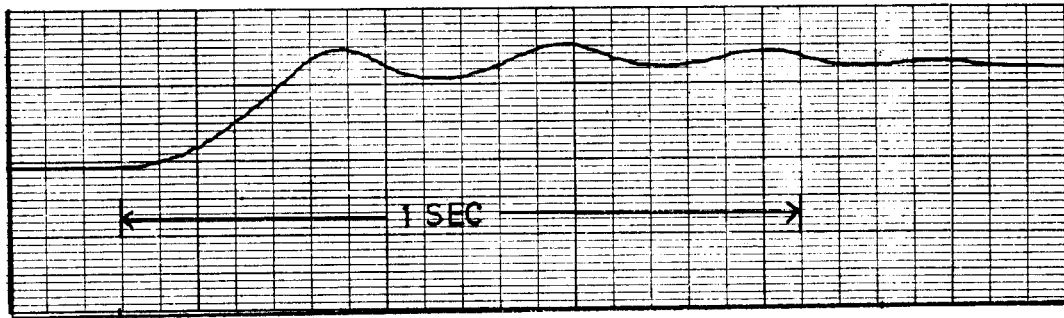


Fig. 10. Step response of the container.

Referring to Fig. 10, the maximum overshoot θm is 0.125 and the period T is 0.12 second. Substituting these values to the following equations³⁾

$$\theta m = e^{-\pi\varphi/\sqrt{1-\varphi^2}}, \quad W_n\sqrt{1-\varphi^2} \cdot T = \pi$$

we have $\varphi = 0.55, \quad W_n = 31 \quad (\text{rad/sec}).$

Hence the container sphere transfer function $G_c(S)$ can be written as

$$G_c(S) = \frac{31^2}{S^2 + 2 \times 0.55 \times 31S + 31^2} \dots\dots\dots (15)$$

Summarizing the theoretical analysis and the experimental result of each element described hitherto, we are to deduce the over-all transfer function for the system.¹⁰⁾

As described in chapter I, in case the sensitive part is settled and contains no transient error in the north-directing function, there is no azimuthal movement of the gyro sphere. As this leads the desired input for the system to be constant, it can be assumed that in practice the reference input for the follow-up system is zero.¹¹⁾

Hence, during normal operating state, only the compass card deflection which is referred to an external disturbance, due to the azimuthal displacement of the stationary part, is assumed to enter the system through the comparator (error detector) directly.

Therefore, we have the following over-all block diagram for the system,

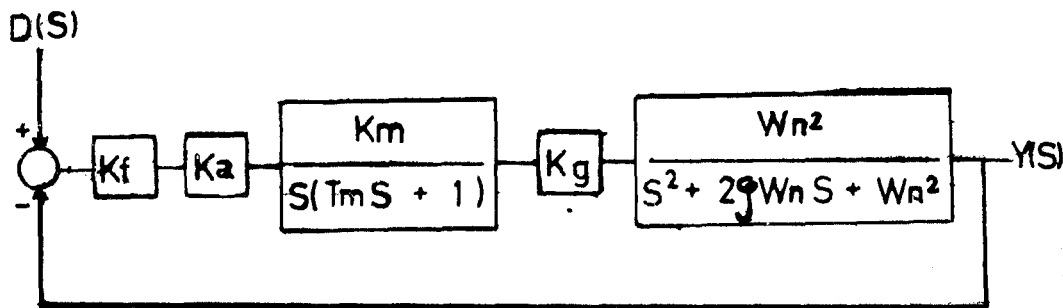


Fig. 11. Over-all block diagram for the follow-up system.

where $D(S)$ denotes the external disturbance(in radian) of the system entering the comparator without any conversion, i. e., the azimuthal displacement of the compass card due to the azimuthal motion of the stationary part and $Y(S)$ denotes the output(in radian), azimuthal displacement of the container sphere due to the follow-up action.

Referring to Fig. 11 the closed loop transfer function can be written as

$$\frac{Y(S)}{D(S)} = \frac{K}{S(Tm S + 1) (S^2 + 2\phi Wn S + Wn^2) + K} \dots\dots\dots(16)$$

where $K = Kf \cdot Ka \cdot Km \cdot Kg \cdot Wn^2$

$$Kf = (4.5 - \frac{3}{4}Ka) \times 57.3$$

$$Ka = 0.06 \sim 1.5$$

$$Kg = 1 / (7 \times 2\pi \times 57.3)$$

$$Km = 30.5 / \{0.12 + (0.024/57.3) \cdot Vc\}$$

$$Tm = 0.03 / \{0.12 + (0.024/57.3) \cdot Vc\}$$

$$Wn = 31$$

$$Vc = Kf \cdot Ka$$

III. EXPERIMENTAL OBSERVATIONS AND NUMERICAL CALCULATIONS

III -1. EXPERIMENTAL OBSERVATIONS

After the servomotor is rejoined to the system and the compass card is settled, the step input is applied to the system as follows: Keeping the gyro compass in normal operating condition, one of the accessible gears is forced to deflect the compass card by two degrees and to be held till the servomotor control voltage reaches the anticipated value by adjusting the gain knob provided on the amplifier. Then the system is released free so that the followup mechanism may act to follow up the gyro sphere.

The indicial responses corresponding to the step inputs are measured as in the same way as described in Chapter II-2, (4). These responses are taken as the observed over-all outputs for the system and illustrated in Fig. 12. The characteristics of these outputs are not smooth. It may be due to the effects caused by the backlashes such as those of gears and spring pinch of link mechanism. The oscillation period of outputs has a tendency to become shorter as K_a becomes higher. The range of oscillation period is between 1 and 2.3 seconds approximately [Fig. 12(a)-Fig. 12(e)]. It is shown that if K_a is smaller than 0.03, the system does not work and if it is over 1.5 it has a sustained oscillation.

III -2. NUMERICAL CALCULATIONS

On dividing both denominator and numerator of right side of Eq. (16) by T_m , we have

$$\frac{Y(S)}{D(S)} = \frac{A(1)}{S^4 + A(4)S^3 + A(3)S^2 + A(2)S + A(1)} \dots\dots\dots(17)$$

where $A(1) = K/T_m$
 $A(2) = W_n^2/T_m$
 $A(3) = W_n(2\phi + T_m W_n)/T_m$
 $A(4) = (1 + 2\phi W_n T_m)/T_m$.

Eq. (17) can be reverted to a fourth order linear differential equation as Eq. (18),

$$\frac{d^4 y(t)}{dt^4} = A(4) \frac{d^3 y(t)}{dt^3} + A(3) \frac{d^2 y(t)}{dt^2} + A(2) \frac{dy(t)}{dt} + A(1)y(t) = A(1) \cdot d(t) \dots(18)$$

where $y(t)$ and $d(t)$ are the inverse Laplace transform of $Y(s)$ and $D(s)$ respectively. From Eq.(18), the dynamical-equation description of the system is to be derived by four state variables⁽²⁾. Let the output y and its derivatives y', y'', y''' be state variables:

$$\begin{aligned} y(t) &= Y(1) \\ y'(t) &= Y'(1) = Y(2) \\ y''(t) &= Y'(2) = Y(3) \\ y'''(t) &= Y'(3) = Y(4) \end{aligned}$$

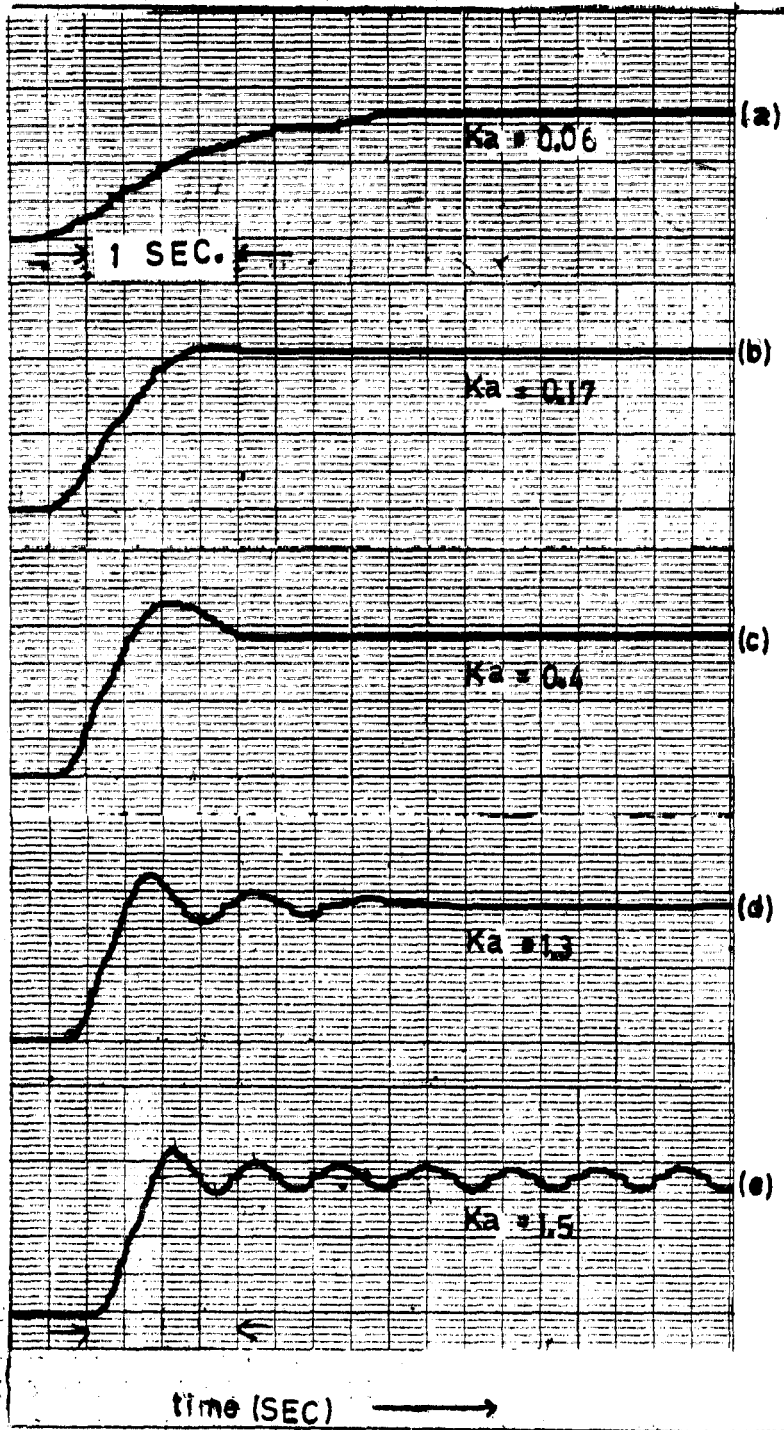


Fig. 12. Observed over-all step response

Differentiating both sides of these equations, we have the following first order simultaneous differential equations.

$$\frac{dY(1)}{dt} = Y(2)$$

$$\frac{dY(2)}{dt} = Y(3)$$

$$\frac{dY(3)}{dt} = Y(4)$$

$$\frac{dY(4)}{dt} = -A(1)Y(1) - A(2)Y(2) - A(3)Y(3) - A(4)Y(4) + A(1)d(t)$$

or

$$\begin{pmatrix} \frac{dY(1)}{dt} \\ \frac{dY(2)}{dt} \\ \frac{dY(3)}{dt} \\ \frac{dY(4)}{dt} \end{pmatrix} = \begin{pmatrix} 0 & 1 & 0 & 0 \\ 0 & 0 & 1 & 0 \\ 0 & 0 & 0 & 1 \\ -A(1) & -A(2) & -A(3) & -A(4) \end{pmatrix} + \begin{pmatrix} Y(1) \\ Y(2) \\ Y(3) \\ Y(4) \end{pmatrix} + \begin{pmatrix} 0 \\ 0 \\ 0 \\ A(1) \end{pmatrix} \cdot d(t)$$

$$Y = [1 \ 0 \ 0 \ 0] \begin{pmatrix} Y(1) \\ Y(2) \\ Y(3) \\ Y(4) \end{pmatrix} \dots\dots\dots (19)$$

Eq. (19) is solved numerically by the digital computer using the Runge Kutta method for various Ka with the initial conditions; Y(1)=Y(2)=Y(3)=Y(4)=0, d=2 degrees=0.01745×2 rad., time increment=0.01 sec., time intervals=10 sec. The values of Y(1) versus time increment are taken as the simulated over-all outputs of the system, which are shown in Fig. 13.

Referring to Fig. 13, the dashed lines indicate the characteristics of the simulated outputs and the solid lines do those of the observed over-all outputs. There is a slight difference in the phase angle between both lines, which is thought to be due to the mechanical backlashes as previously described.

IV. CONCLUSIONS

Through the theoretical analysis and experimental observation of each element contained in the follow-up mechanism of Hokshin D-1 gyro compass, five transfer functions are deduced separately. From them an over-all closed loop transfer function is derived and a mathematical model for the control function is proposed with the intention of systematical researching of the optimal control and of studying on the fundamentals for a gain adjusting guide of the follow-up control system.

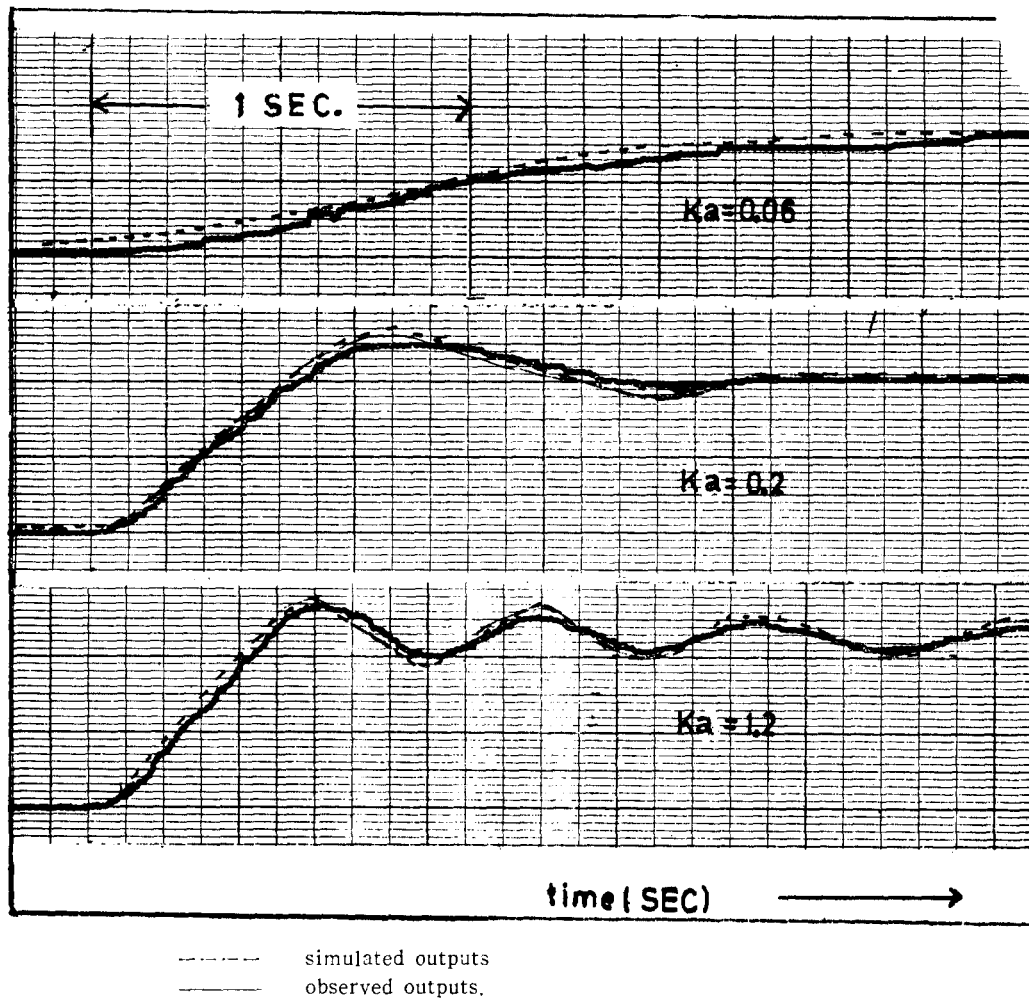


Fig. 13. Comparison of over-all step responses of observations and those of simulations.

The principal results of this paper are summarized as follows: Under the normal operating condition, the adjustable range of the amplification factor, K_a is between 0.03 and 1.5 and the servomotor angular velocity is less than 2,500 r.p.m. While the actuating signal voltage is directly proportional to the deflection angle for a given K_a , it is also characterized by a linear equation with negative slope of K_a for a given deflection angle. While servomotor control voltage is directly proportional to the deflection angle for a given K_a , it is also characterized by a second order equation of K_a , having a positive derivatives in the range of a adjustable K_a , for a given deflection angle. The follow-up system shows a slight oscillation response for a step input. The higher is the K_a , the shorter the oscillating period. By considering the fact that the external disturbance enters the system through comparator directly without any conversion and reference input is zero in normal operation state, the system can be expressed as a strictly proper type transfer

function and modeled in the fourth order linear differential equation. The characteristics of the over-all outputs by the digital computer appeared to be well consistent with those of the experimental results, if the effects of coulomb friction and mechanical backlashes such as those of gears and spring pinches of linkages are disregarded.

The system representation proposed in this paper is expected to be a powerful means of analysis of the control system on the different types of similar gyro compasses.

Acknowledgements. I wish to express my gratitude to profs. Chi-won Chang, Joo-shik Ha and Hong-sun You for the extensive discussions and encouragements during this research. I am particularly grateful to prof. Cheol-yung Lee, who originally suggested the value of the study on the optimal control of the follow-up system on the ships' gyro compass and gave me the computer program for obtaining the simulated over-all outputs. I am also indebted to profs. Se-mo Chung and Bae-yung Pak for their kindness in reading the manuscript critically and suggesting numerous improvements.

REFERENCES

- 1) Norbert Kliemann, Rechnergestutzter Kreiselkompass, Fabrik Nautischer Inst., p.14, Hamburg, 1974.
- 2) J. Klinkert, The Ships' Compass, p.474, Routledge and Kegan Paul Ltd, 1970.
- 3) M. Kushida, Test Reports on the Characteristics of the signal and output voltage for Hokshin D-1 gyro compass, Hokshin Electric works Ltd., 1968.
- 4) Ohm, Control Components Manual, p.VIII-154, Ohm, 1968.
- 5) George J. Thaler, Servomechanism Analysis, p.124, New York, 1970.
- 6) Francis H. Raven, Automatic Control Engineering. pp.10-11, McGraw Hill, 1971.
- 7) Feynman, Lectures On Physics, Vol. II. p.38-6, Addison-wesley pub., 1968.
- 8) Lamb, Hydrodynamics, pp. 571-641, Cambridge University Press, 1970.
- 9) Nagada Dagashi, Theory of Automatic Control, p.187, Ohm, 1965.
- 10) Naebada, Control Systems for the Navigation, p.28, Japan, 1970.
- 11) Joo-shik Ha, Automatic Control Engineering, p.90, 1976.
- 12) C.T. Chen, Introduction to Linear System Theory, p.89, Winston, 1970.